METAL COVERAGE ON SINGLE-WALL CARBON NANOTUBES : METAL NANORING AND NANOTUBE FORMATION

A THESIS

SUBMITTED TO THE DEPARTMENT OF PHYSICS

AND THE INSTITUTE OF ENGINEERING AND SCIENCE

OF BILKENT UNIVERSITY

IN PARTIAL FULFILLMENT OF THE REQUIREMENTS

FOR THE DEGREE OF

MASTER OF SCIENCE

By

V. M. Kemal Bağcı

June 2002

I certify that I have read this thesis and that in my opinion it is fully adequate, in scope and in quality, as a dissertation for the degree of Master of Science.

Prof. Dr. Salim Çıracı (Supervisor)

I certify that I have read this thesis and that in my opinion it is fully adequate, in scope and in quality, as a dissertation for the degree of Master of Science.

Prof. Dr. Atilla Erçelebi

I certify that I have read this thesis and that in my opinion it is fully adequate, in scope and in quality, as a dissertation for the degree of Master of Science.

Prof. Dr. Şinasi Ellialtıoğlu

Approved for the Institute of Engineering and Science:

Prof. Mehmet Baray,
Director of Institute of Engineering and Science

ABSTRACT

METAL COVERAGE ON SINGLE-WALL CARBON NANOTUBES : METAL NANORING AND NANOTUBE FORMATION

V. M. Kemal Bağcı
M. S. in Physics
Advisor: Prof. Dr. Salim Çıracı
June 2002

The carbon nanotubes are welcomed as the basis element for electronic and opto-electronic devices of nanometers size, the size of a few atoms. The question of crucial importance in the physics of utilization of nanotubes as nanowires, transistors, couplers etc. is the metal-nanotube interactions. In this thesis, we considered the problem of metal coverage of nanotubes and single atom-metal interactions, using the first-principles computational techniques. We had found that Ti, Fe and Ni bind strongly to the nanotube while Al, Cu and Au has weak binding. We propose that d orbital electrons of transition metal elements play important role in the strong interactions. We also observed that strong metal-metal interaction prevents uniform coverage of nanotube, however a stable ring and tube of aluminum atoms with well defined patterns can also form around the semiconducting SWNT's and lead to metallization. We have obtained a criteria for the uniform coverage of nanotubes by metal atoms.

Keywords: Nanotubes, carbon, metal coverage, metal ring, metal tube, binding, ab-initio electronic structure.

ÖZET

TEK ÇEPERLİ KARBON NANOTÜP ÜZERİNE METAL KAPLANMASI: METAL NANOHALKA VE NANOTÜP OLUŞUMU

V. M. Kemal Bağcı
Fizik Yuksek Lisans
Danışman: Prof. Dr. Salim Çıracı
Temmuz 2002

Karbon nanotüpler nanometre boyutundaki elektronik ve opto-elektronik aygıtların gerçekleştirilebilmesi için ideal bir malzeme olarak kabul edilmektedir. Bu tür sistemlerin fiziğinde en temel soru metal-nanotüp etkileşimleridir. Bu tezde, nanotüplerin metal kaplanması ve tek atom-nanotüp etkileşimlerini inceledik. Ti, Fe ve Ni atomlarının nanotüpe kuvvetli ve Al,Cu ve Au atomlarının ise zayıf bağlandığını gözlemledik. Geçis elementi metallerinin d orbitallerinin bu noktada önemli bir rol oynadığını öne sürüyoruz. Ayrıca, metal-metal etkileşimlerinin nanotüp yüzeyinin eşdağılımlı kaplanmasını engellediğini, buna karşın tüp etrafında alüminyum atomlarından oluşan ve belirgin şekle sahip halka ve tüp oluşabildiğini ve bunun metalleşmeye yol açtığını gösterdik. Nanotüpün eşdağılımlı kaplanması için bir kriter öne sürdük.

Anahtar sözcükler: Nanotüpler, karbon, metal kaplama, metal halka, metal tüp, bağlanma, ilk-prensipler elektronik yapı

ACKNOWLEDGMENTS

I would like to present my greatest respect and thanks to Prof. Salim Çıracı for his guidance and patience.

I would also remember the support by Dr. Oğuz Gülseren and Dr. Taner Yıldırım and their corporation with gratitude.

I would like to give my special thanks to Sefa Dağ for his assistance and discussions.

I would like to thank my family for trusting me and keeping their support.

And finally, I would like to devote this work to my dear wife Eylem, without whom any effort would be meaningless...

Contents

List of Figures

List of Tables

Chapter 1

INTRODUCTION

The carbon element, in numberless different structures and compositions, has always attracted the interest of human mind. From the sparkle of diamond, to the fuel we burn, and in many raw materials we use in forms of fibers, polymers etc., carbon is everywhere in our life. The research in carbon and its structure has always been open to new discoveries and surprises.

The year 1991, at the onset of wave of other strange carbon structures like fullerenes, has yielded a very interesting new form of carbon, the carbon nanotube. In those years, people were interested in obtaining strong and reliable carbon fibers, and their properties. Kubo[1] speculated about the limits of the size of the carbon fibers. He and Smalley discussed about the probable structure and properties of this limit size small fiber and thought that it would be something like a C_{60} or C_{80} spherical shaped molecule elongated, forming a cylinder of a few nanometers in diameter. Dresselhaus[2] has suggested how zone folding could be used to examine the electron and phonon dispersion relations of these theoretical tubes. Mintmire *et al.*[3] has gone further, and predicted among many things that these tubes might have carrier densities similar to that of metals. They also predicted that the tube, being a 1-D system, will have no Peierls distortion (bond alternation in order to lower energy, resulting in the formation of a band gap). However the real breakthrough on nanotube research came with Iijima's[4] report on the experimental observation of carbon nanotube using TEM. The

carbon nanotube is a honeycomb lattice of carbon rolled into a cylinder, with a diameter of nanometer size. It might be several μm long, capped at the ends by semi-spherical structure made of pentagons, hexagons or heptagons. The length/diameter ratio is very high, so at the middle, the tube can be considered as flawless cylinder extending to infinity. A detailed explanation of the structure and physical properties of carbon nanotubes will be given in Chapter 2.

Carbon nanotubes, hereafter referred as nanotubes (NT) only, are fantastic materials with enormous stability and elasticity but they have very high Young's modulus, that is, it is easy to apply elliptical deformations but is very difficult to elongate the system. It is shown that they have exceptionally large and reversible volume reduction capacity (very high compressibility)[5,6]. The stable structure of NT allows bending, stretching etc. at will, without any elastic deformation.

Nanotubes have radius and structure dependent physical properties[7,8,9]. They can be either metallic or semiconducting depending on the chirality and radius. A simple zone-folding explanation for the metallicity of nanotubes is given also in Chapter 2. Recent research[10,11,12] demonstrates the dependence of band gap of semiconducting nanotubes on radial deformations. These deformations are also reversible.

The exceptional properties of nanotubes can be exploited in numerous applications[9,13]. They can be used as bare tubes, or may be doped, covered or intercalated with different atoms; molecules attached, adsorbed etc. A few examples of the probabilities will give the reader enough, but nevertheless incomplete by its nature, idea of the wide range of applications and physical interest for nanotubes.

The use of nanotubes in technologies related to microscopy is an already realized application. Dai *et al.*[14] pionered the use of nanotubes for SPM (scanning probe microscope) tips as a postdoc with Smalley at Rice University. Nanotubes are chemically inert and mechanically robust, have a large aspect ratio and have a in principle well-defined tip. Stanislaus Wong and his coworkers in Lieber's group at Harvard have developed methods to chemically functionalize the very end of nanotube.

Aranson[15] and his coworkers have demonstrated that the use of nanotubes as tip extensions enhanced the resolution for electrostatic microscopy. The same physical properties mentioned above make nanotube a good candidate for use as a tip for AFM (atomic force microscope).

The utilization of nanotube capillary is also possible. The tubes may be used as nanocontainers, for various atoms and molecules. The adsorption of nanotubes may be tuned on both inside and outside by deformations[16]. Various studies have also shown that pressure induced modifications of capillary fillings for crystal structure (rope or bundle of nanotubes) is possible. This means that the atoms or molecules may be trapped or adsorbed inside nanotubes, and released at will with changes in applied pressure, or temperature.

Using nanotubes as field-emitter tips is one promising possibility. Yahachi Saito and his coworkers at Mie University in Japan developed cathode-ray tubes equipped with nanotube field emitters[17]. This has applications in color displays replacing the metallic emitter tips.

The use of nanotubes will be most striking in the field of electronics, paving the way to the realization of nanoelectronics. The size of a nanotube is order of hundreds times smaller than the state-of-the art commercial circuit elements. The question is, can the nanotubes be used as basis for electronic devices? The observed or predicted properties of nanotubes claim so.

The nanotube as a material do not have a strict electronic structure. As mentioned before, the geometry of nanotubes determine the structure in a reversible manner. But geometry is not the only factor that determines how electrons behave inside the tube. Doping the nanotubes, for example with alkali atoms, have drastical effects on the electronic structure. The fact is that, such modifications like deformations or doping regions might reside on segments of nanotubes, for example making them semiconducting, while the other segments remain metallic. This creates the opportunity of establishing a Schottky barrier along the tube axis.

Chico and his coworkers[9] have predicted a quantum dot formation on nanotube by creating defects of pentagon-heptagon pairs. They will act as

scattering centers for electrons. The existence of a quantum dot structure opens new opportunities for devices, because these regions will bring 1-D electron confinements.

The use of molecular structure, like nanotubes, in electronics is a field so called molecular electronics. In 1998, Tans *et al.*[17] have reported the fabrication of a field-effect transistor, made of one semiconducting single-wall carbon nanotube (SWNT), connected to two metal electrodes. By applying a voltage to gate electrode, the nanotube can be switched from a conducting to an insulating state. Electrical measurements on the nanotube transistor indicate that its operation characteristics can be qualitatively described by semiclassical band-bending models for traditional semiconductor devices. A similiar report at the same year was also given by Martel *et al.*[18]

The property of the nanotube, of utmost importance for the scope of this thesis, is the conductance of nanotubes. The existence of a metallic state in nanotubes as a 1-D system, in contrast to the predictions of Rudolf Peierls, is a novel property of the nanotube structure. The existence of conductance in nanotubes have many times been observed experimentaly. The 4-probe resistance measurements by Ebbesen and his coworkers[19] yielded resistance values from $100\,M\Omega$'s to several $G\Omega$'s (per meter). In the same year, Dai *et al.*[20] have found out resistance values again about several $G\Omega$'s for individual nanotubes. Note that these values are given for individual bare SWNT's (and resistance for a typical length of $1\,\mu m$ is about $10 - 100\,k\Omega$'s). The resistance of metallic nanotubes on the order of hundreds of $M\Omega$'s per meter was observed in several other experiments[22,23]. These values correspond to resistivities down to $\sim 10^{-5}\,\Omega cm$, almost comparable to that of typical metals. The resistance of metallic nanotubes is good enough for using them as nanowires but the story doesn't end here.

The occurance of quantum conductance for SWNT's was observed[21] very recently. The researchers in Stanford University have found that SWNT's exhibits quantum conductance, in the order of $10G_0$'s for nanotubes they observed , where $G_0 = \frac{2e^2}{\hbar^2}$ is the unit quantum conductance. Due to the limited size and low

density of states at the Fermi level, nanotubes are not suitable for carrying large currents. But a more important obstacle to the application of nanotubes in electronic devices is high resistance of electrical contacts to nanotubes[17,18,24], called contact resistance. The nanotube based devices will be most useful if they can be made very small and fast, with low power dissipation. All of these require low contact resistance. The importance of contact resistance compared to nanotube resistance is evident from $1-4\,M\Omega$ resistance of metal-nanotube contact to $1-100\,k\Omega$ resistance of a $1\,\mu m$ long nanotube. One important remark here will be that the typical metal-metal contact resistance will be of the order of the quantum resistance $R_c = \frac{h}{2e^2} \sim 13k\Omega$. The situation of nanotube based devices looked bleak, however it was not as hopeless as it was thought.

The previously fabricated metal contacts were either Pb or Au contacts. The resistance of a Ti contacted metallic SWNT was reported to be as low as $12\,k\Omega$'s for several microns tube length[25]. This indicates a significantly low metal-nanotube contact.

The importance of metal-nanotube interaction on molecular electronics, from the point of view of realizing nanotube based devices, is not only limited to contact resistance problem. It is also possible to devise high conductance metallic nanowires by coating the sidewalls of nanotubes by metals. Such nanowires will replace current metal wires in the future devices, because they are very stable and small at the same time. You can bend these wires at will to make your connections.

The problem of metal coverage and metal-nanotube interaction had begun to attract increasing attention in time. Two recent research in the year 2000 has experimentally observed the coating of metal atoms around nanotubes[26,27]. They have coated various metals on SWNT's suspended between gold grids, so except the hanging regions, the nanotubes are in the air. Among the metals coated are Ti, Al, Au, Fe, Ni and Pd. The coating on nanotubes were up to thicknesses of 0.5, 5 and 15 nm's. The experiments revealed that the metal coatings differed in smoothness and in shape for each metal. It turned out that, at all coating thicknesses, the most smooth coverage was obtained for titanium. The coating

was continuous and uniform. However for aluminum, gold and iron, the metal atoms formed discrete particles or islands of atoms, like beads suspended on the nanotubes. More interestingly, as long as the coverage thickness increased, the Al, Au and Fe atoms tended to form bigger and more discrete beads.

The researchers who has conducted the experimental work has proposed a well known definition for this phenomena, which is expressed in detail in the book by Chopra[28]. The idea is that in the deposition of a material on a substrate, the structure and morphology of the coating depends on the interactions between the deposited atoms and substrate, and interactions within. For the experimentally observed cases, the metal-nanotube and metal-metal interactions play the important role. The researchers suggest that the interaction between titanium and nanotube is stronger than interaction between titanium atoms. On the other hand, the interaction between aluminum, gold or iron and nanotube is much weaker than interactions within metal atoms.

We had started the theoretical investigation of metal coverage around nanotubes by first asking a crucial question : Is it possible to have a stable metallic structure around the nanotube? The answer to this question will shed light on the metal-nanotube interaction in the sense that, if a stable structure is formed, what is the physical reason for such a formation or vice versa.

The first problem we investigated was the single atom-nanotube interactions. We had calculated the binding energies for various atoms to four plausible binding sites over the nanotube. We looked for an explanation of the strong binding of the transition metal elements.

The next problem we investigated was the formation of a metallic ring of aluminum around nanotube. Various structures for the aluminum ring was tried, in order to check the dependence of stability on the structure.

The final phase was the full coverage of nanotube with metal atoms. This structure would be a metallic sheet of finite thickness and significant conductance. In the experimental work, it was seen that aluminum didn't form a thin film around the nanotube. However, the process of deposition might be misleading because the experiment only shows that the incident aluminum atoms tended

to form clusters sticking to each other, but couldn't clear out whether the structure once formed is stable or not. Again we tried various structures for aluminum coverage and checked the dependence of stability and morphology of the final structure on the initial system structure.The reader may again find more information on the structures and details in Chapter 3.

In all cases, the structures were fully optimized and the ground-state electronic structure was obtained. The first principles total energy and electronic structure calculations were carried out by using pseudopotential plane wave method[29] within density functional theory[30,31]. The results were obtained within the generalized gradient approximation[32] (GGA). Atomic relaxations were done by conjugate gradient method, and structure was fully optimized. The explanations of these methods are given in Chapter 2.

The organization of this thesis is as follows : In Chapter 2, the theoretical background of the calculations is presented. Information on carbon nanotubes and the methodology of calculations is also given in Chapter 2. In Chapter 3, our calculations are presented. The discussion of the results and our conclusion are summarized in Chapter 4.

Chapter 2

THEORETICAL BACKGROUND

2.1 Carbon Nanotube

The carbon atom is the sixth element of the periodic table and is listed at the top of column IV. It has six electrons which occupy $1s^2$, $2s^2$ and $2p^2$ atomic orbitals. Three possible hybridizations of s and p orbitals occur in carbon involving materials, namely *sp*, sp^2 and sp^3. Carbon exhibits *sp* hybridization in Acetylene, HC≡CH; sp^2 hybridization in graphite(graphene is a single-layer of graphite) and sp^3 hybridization in diamond.

The hybridization of carbon depends on the surrounding atoms. It is nothing but the result of energy minimization process. However, once hybridization and accompanying bonding occurs, it is a stable structure. The fact that diamond is the most stable and lowest energy form of carbon doesn't mean that all carbon structures will lead to diamond. Indeed, diamond requires such conditions for spontaneous formation that it is a rare and precious item.

Many forms of carbon structures consisting of only carbon atoms may occur, but these are usually in amorphous structures like in coal. One interesting crystalline form of carbon is the graphite structure. Graphite is in fact a stacking of layers of carbon atoms, called graphene. Graphene is a two-dimensional hexagonal system, with a single carbon at the edges. Each carbon has three neighbors at a distance of $1.42A^0$'s. In graphene, carbon makes sp^2 hybridization

as mentioned before, which couples the $2s$ state with two $2p$ states and these hybrid orbitals make three σ-bonds with the neighbors. Three of four valence electrons of carbon is now shared, the remaining one electron is in the uncoupled $2p$ orbital, which resides perpendicular to the plane of graphene. These orbitals form weaker π-bonds with the neighboring atoms. The band structure of graphene(Fig. 2.1) shows that the π-band mainly determines the solid-state properties of graphene. The band structure reveals that graphene is a zero band-gap semiconductor[33] or a metal with a Fermi surface consisting of a single point.

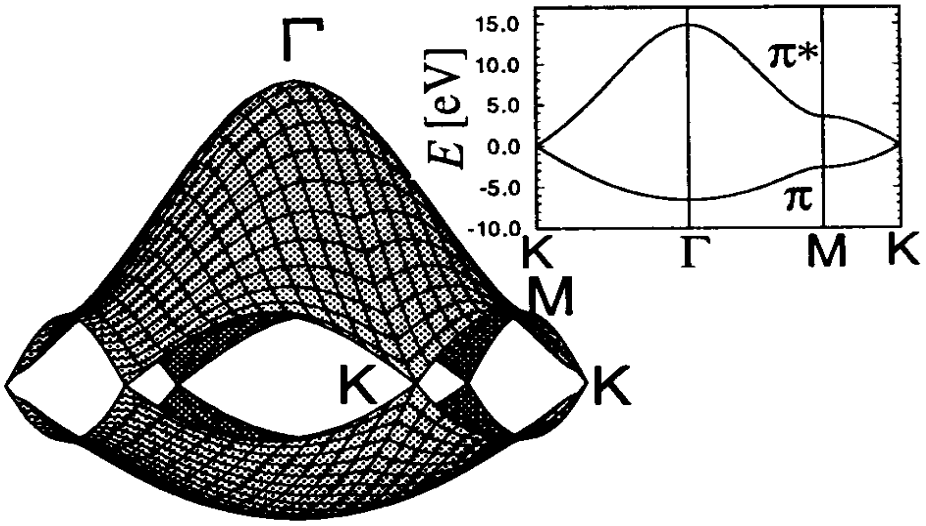

Figure 2.1: The band structure of graphene. The π^* and π bands intersect at point K, which makes graphene a zero band gap semiconductor. [Ref 33]

The reciprocal lattice of graphene can be deduced from the lattice vectors, forming a hexagonal Brillouin zone. The Fermi level crosses the zone boundary at the K-point.

Now consider a graphene sheet cut rectangularly and rolled into a cylinder along an axis, so the terminating atoms at one side match atoms at the other side. The vectors that determine this rectangle is shown(Fig. 2.2). A single-wall carbon nanotube can be described as a graphene sheet rolled into a cylindrical shape so that the structure is one-dimensional with axial symmetry, and in general

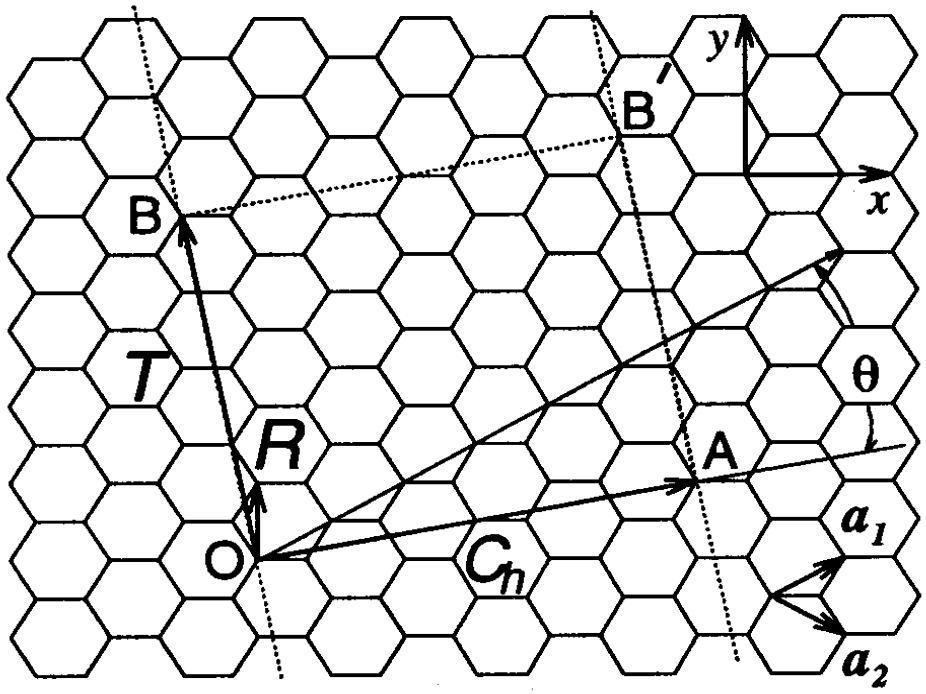

Figure 2.2: The graphene structure and 2D unit cell of nanotube. $OABB^{'}$ rectangle defines the nanotube unit cell. The chiral vector $\vec{C}_h$ and the translation vector $\vec{T}$ are generated from the graphene lattice vectors $\vec{a}_1$ and $\vec{a}_2$.

exhibiting a spiral conformation, called *chirality*[33].

The structure of carbon nanotube unit cell is determined by the chiral vector $\vec{C}_h$. It actually defines how the graphene layer is rolled over. The chiral vector $\vec{C}_h$ is a linear combination of graphene basis vectors $\vec{a}_1$ and $\vec{a}_2$ (Fig. 2.2).

$$\vec{C}_h = n\vec{a}_1 + m\vec{a}_2 = (n, m) \tag{2.1}$$

The (n,n) nanotubes are called armchair, (n,0) as zigzag and (n,m) in general as chiral nanotubes.

The other vector forming the rectangle is the translation vector $\vec{T}$, which is the vector that the nanotube structure repeats itself along the axis, and is obtained from (n,m) as

$$\vec{T} = t_1\vec{a}_1 + t_2\vec{a}_2 \tag{2.2}$$

$$t_1 = \frac{2m+n}{d_R}, t_2 = -\frac{2n+m}{d_R} \tag{2.3}$$

where d_R=d (3d) if n-m is not a multiple of 3d (n-m is a multiple of 3d), introducing d as the greatest common divisor of n and m.

The SWNT is a flawless cylinder that extends to infinity(Fig. 2.3), but of course the real nanotube is terminated at the ends by semi-spherical structures. The typical length of nanotubes produced so far is about $1\mu m$. The diameter of the carbon nanotube, d_t, is given by,

$$d_t = \frac{|\vec{C}_h|}{2\pi} = \frac{a\sqrt{n^2+m^2+nm}}{\pi} \tag{2.4}$$

where the lattice constant of honeycomb lattice (graphene 2-D lattice) a=$2.49A^0$. The diameter of the most commonly produced nanotubes is between 0.5nm and 2.0 nm's, with typical length/diameter ratio over 1000.

The geometry of the nanotube is related to the lattice of graphene 2-D structure, and it is also possible to deduce other physical properties, in particular the electronic structure from the band structure of graphene. The rolling of graphene on a cylindar is a periodic boundary condition imposed on the system, in the direction of $\vec{C}_h$. You might consider this as increasing the size of the cell $|\vec{C}_h|$ times in that direction. The result of this is the creation of discrete wavevectors, that is the projection of the wavevector $\vec{k}$ on the reciprocal lattice vector $\vec{K}_1$ has discrete values(Fig. 5). The electronic structure for nanotube can be deduced by zone-folding method from graphene electronic structure.

As one can see from the figure, depending on (n,m), the discrete energy states might fall over K point on the graphene Brillouin zone, where the Fermi level resides. In other words, there occurs non-zero density of states at the Fermi level, which makes the system metallic. The condition that satisfies the fact that there is non-zero density of states at Fermi level is found as;

- n=m (armchair nanotubes)
- 2n+m is a multiple of 3

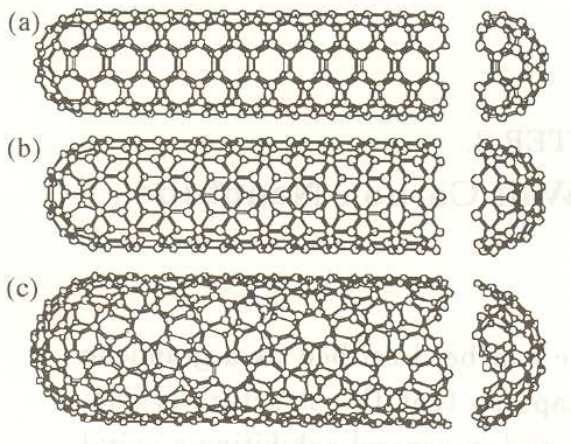

Figure 2.3: The geometry of carbon nanotube. The caps at the end of the tube has the structure of fullerene.

This simple zone-folding method has its shortcomings due to the curvature effects of the carbon nanotubes. The uncoupled p orbitals in the graphene structure which forms weak π-bonds now has significant overlap with neighboring atomic orbitals at the inner side of the nanotube. Because of this overlapping (or π^*-σ^* hybridization), the structure is further stabilized and the electronic properties change. Indeed, ab-initio calculations have shown that[34] for some high curvature nanotubes, very small band-gap semiconductivity occurs instead of metallicity. The zigzag (9,0) SWNT which is predicted to be a metal is in fact a small band gap semiconductor.

Initially, carbon nanotubes are discovered as multiwalled tubes (MWNT). SWNT's are synthesized subsequently. Actually, Iijima had found[4] another type of nanotube, the multi-wall nanotube (MWNT). MWNT is a group of SWNTs found inside each other. The outer nanotube surrounds other nanotubes with smaller radii (Fig. 6). The interaction between SWNTs in the MWNT structure is found to be weak, presumably originating from Wan-der-Walls interaction as in the case of interactions between graphene layers in graphite structure.

The synthesis of SWNT's initially was a by product of synthesis of MWNT's,

and in fact the experimental observation of SWNTs had to wait until 1993, when Iijima *et al.*[35] and Bethune *et al.*[36] had independently reported their observations. The research in SWNTs had flourished after the discovery of a method by Thess *et al.*[37] that yielded high efficiency SWNT synthesis. This method uses a laser beam to evaporate a target containing carbon mixed with a small amount of catalyst metals Co or Ni. The vapor is blew over a cooled Cu collector by Argon gas flow and condensates on the collector, giving ropes of SWNTs. This rope consists of several SWNTs, which wind around each other, later to be seperated.

Another method of SWNT synthesis is the arc discharge method[38]. The rods of graphite are used as electrodes and a very high current is passed (about 100 amperes). The nanotubes are formed on the negative electrode. By the use of transition metals as catalysts, SWNT formation with a 20% yield is possible.

The most recent and most controllable growth technique for the synthesis is the chemical vapor deposition (CVD) method. Soh *et al.*[39] had discovered a method of high quality SWNT fabrication on catalyst patterned surfaces. This method allows large amount of SWNT yields at specified positions. Use of subsequent mask etched by electron beam lithography is used to collimate vapors of CH_4. The development of synthesis techniques allows growth of SWNTs in significant amounts. However it is still not possible to fabricate nanotubes with a specified (n,m) values at will. On the other hand, characterization of nanotubes (determination of chirality etc.) using TEM or AFM techniques is well established.

2.2 Methodology

The physical properties of interest in any system concerning solid state physics problems involves electronic structure, the total energy of ion-electron system, phonon dispersion relations, other excitation properties and eventually engulfing all, the geometric structure. The quantum theory is a well established theory that explains the physics of these system in a profound manner and it has been proven to be correct to very high precision in many cases. The exact solution

of quantum mechanical equations will give precise information on the system, including the total energy of the electrons and nuclei.

The physical properties of any system, nearly all of them, are related to the total energy or to the differences between total energies[29]. For instance, the equilibrium lattice constant of the crystal is the lattice constant that minimizes the total energy. If you can determine the total energy as a function of a parameter, you can find the equilibrium value of the parameter by minimizing the energy with respect to the it.

As mentioned before, the total energy of the system might be calculated by solving quantum mechanical equations. However, for a very large system comprising of many atoms, ions and electrons, the analytical solution to these equations is impossible. The complexity of the equations and high numbers of variables impose tremendous obstacles for even an exact computational solution.

2.2.1 The Adiabatic Approximation

In order to treat the problem, various approximations have to be made, because of the tremendous number of particles (electrons and ions) comprised in a small size of solid material. Every approximation introduced to the system moves it further away from the exact solution, however clever choices for the approximations build upon physical facts will minimize these deviations.

The first approximation to system consisting of ions and electrons, as in our case, comes from the large mass difference between nuclei and the electrons. Because of the large difference in mass, electrons respond essentially instantaneously to the motion of the nuclei. Thus the nuclei can be treated adiabatically, leading to a separation of electronic and nuclear coordinates in the many body wavefunction. This approximation is called the Born-Oppenheimer approximation. This reduces the problem into solving electronic wavefunctions in a frozen configuration of the nuclei, at any instant of the system.

2.2.2 Hartree-Fock Approximations and Density Functional Theory

The second and the most important approximation, is the single-electron model and the density functional theory. The electron-electron interactions for such big and complicated systems are impossible to solve analytically. The reason for that is the wave function of the electronic system depends on the potential due to electron-electron interaction which depends on the wave function itself, other then the large number of electrons imposing many coupled differential equations.

The many particle wave function is a coupled function of the coordinates of many particles. It obeys the Schrödinger equation given below,

$$\left[-\frac{\hbar^2}{2m}\sum_i {\nabla_i}^2 + \sum_i V_{ion}(\vec{r}_i) + \frac{1}{2}{\sum_{i,j}}' \frac{e^2}{|\vec{r}_i - \vec{r}_j|}\right] \Psi(\vec{r}_1, \vec{r}_2, ...\vec{r}_N) = E\Psi(\vec{r}_1, \vec{r}_2, ...\vec{r}_N) \tag{2.5}$$

where E is the total energy and $\Psi(\vec{r}_1, \vec{r}_2, ...\vec{r}_N)$ is the wave function. This equation is correct for understanding almost all of the properties of the solids however, because of the electron-electron interaction, the equation can not be separated to obtain independent equations in the coordinates of the individual electrons.

If the Hamiltonian of the system could be written as the sum of individual Hamiltonians depending only upon the individual coordinates, the total wave function could be written as the product of one-electron wave functions each depending on the coordinates of one electron, such that

$$\Psi(\vec{r}_1, \vec{r}_2, ...\vec{r}_N) = \psi_1(\vec{r}_1)\psi_2(\vec{r}_2)...\psi_N(\vec{r}_N) \tag{2.6}$$

where $\psi(\vec{r}_i)$ denote the wave function for the ith electron. Though Hamiltonian can not exactly be separable, Hartree suggested a variational calculation in which the the wave function is approximated by such a product and the energy, $\langle\Psi|H|\Psi\rangle/\langle\Psi|\Psi\rangle$, is minimized. Even if the wave function is not so accurate, the energy would be a good approximation.

This variational procedure leads directly to the Hartree equations from which

the one-electron functions that minimize the energy may be determined[46].

$$\left[-\frac{\hbar^2}{2m}\nabla^2 + V(\vec{r}) + \sum_j{}' e^2 \int \frac{\psi_j^*(\vec{r'})\psi_j(\vec{r'})}{|\vec{r}-\vec{r'}|} d^3\vec{r'}\right]\psi_i(\vec{r}) = \epsilon_i\psi_i(\vec{r}) \tag{2.7}$$

The sum is over all occupied states, except the state ψ_i. The Hartree equations are one-electron equations in which the potential seen by each electron is determined from the avarage distribution $\sum_j{}' \psi_j{}^*(\vec{r'})\psi_j(\vec{r'})$ of all of the other electrons. The ϵ_i are variational parameters that are in form of one-electron energy eigenvalues. However, their sum is not the total energy, as can be seen from,

$$\frac{\langle\Psi|H|\Psi\rangle}{\langle\Psi|\Psi\rangle} = \sum_i \epsilon_i - \frac{1}{2}\sum_{i,j}{}' e^2 \int \frac{\psi_j^*(\vec{r'})\psi_j(\vec{r'})\psi_i^*(\vec{r})\psi_i(\vec{r})}{|\vec{r}-\vec{r'}|} d^3\vec{r}d^3\vec{r'} \tag{2.8}$$

because we have counted the interaction between each pair of electrons twice.

In the Hartree approximation, we have omitted the indistinguishability of the electrons. Since electrons are identical particles and fermions, the wave function in total including spin should be anti-symmetric with respect to an exchange of two electrons. The corresponding wave function may be written as a Slater determinant,

$$\Psi(\vec{r}_1,\vec{r}_2,...\vec{r}_N) = \begin{vmatrix} \psi_1(\vec{r}_1) & \psi_1(\vec{r}_2) & ... & \psi_1(\vec{r}_N) \\ \psi_2(\vec{r}_1) & \psi_2(\vec{r}_2) & ... & \psi_2(\vec{r}_N) \\ ... & ... & ... & ... \\ \psi_N(\vec{r}_1) & \psi_N(\vec{r}_2) & ... & \psi_N(\vec{r}_N) \end{vmatrix} \tag{2.9}$$

and we may again apply the same minimization principle and this time reach the Hartree-Fock equations,

$$\left[-\frac{\hbar^2}{2m}\nabla^2 + V(\vec{r}) + \sum_j e^2 \int \frac{\psi_j^*(\vec{r'})\psi_j(\vec{r'})}{|\vec{r}-\vec{r'}|} d^3\vec{r'}\right]\psi_i(\vec{r}) \underbrace{-\sum_j e^2\psi_j(\vec{r})\int \frac{\psi_j^*(\vec{r'})\psi_i(\vec{r'})}{|\vec{r}-\vec{r'}|} d^3\vec{r'}}_{exchange\ interaction} = \epsilon_i\psi_i(\vec{r}) \tag{2.10}$$

The extra term in the Hartree-Fock equations, other than the direct interaction term which is also present in the Hartree approximation is called the exchange interaction. This term comes from the anti-symmetry condition and it reduces the total energy of the system, by producing a separation between electrons of same spin, which decreases the positive Coulomb interaction however at the cost of increasing the kinetic energy.

There is also one more effect, called the correlation effect, which occurs due to the separation between electrons of opposite spin. This term is extremely difficult to calculate for bulk solid systems, but nevertheless some methods have been introduced to handle that problem.

The density functional theory DFT, developed by Hohenberg and Kohn[44], and Kohn and Sham[45], has provided a way to solve the problem of many electron system. Hohenberg and Kohn proved that the total energy, including exchange and correlation, of an electron gas even under the influence of an external static potential, for our case the potential due to ions, is a unique functional of the electron density. Further, the minimum value of the total energy functional is the ground-state energy of the system, and the density that yields this minimum value is the exact ground-state energy. In addition to this, Kohn and Sham showed how to replace the many-electron problem by an exactly equivalent set of self-consistent one electron equations. Self-consistent here means that the solutions determine the equations themselves.

The important distinction between Hartree-Fock approximation and the Hohenberg-Kohn theory is the initial approach to the problem. Hartree-Fock method initially approximates a set of single-electron wave functions, anti-symmetrized by the Slater determinant approach and minimizes the total energy in terms of these functions. However, in the density functional theory, the total energy is introduced as a functional of the charge density, which is introduced ad-hoc to the system. The charge density later is definable as the sum of single-electron densities, whence the derivation of total energy with respect to the charge density yields the Kohn-Sham equations. In fact, such an introduction of the charge density will allow calculation of exchange-correlation effects as a

functional of charge density, which might be deduced from some approximative methods, like the local density approximation[45,47] or the generalized gradient approximation.[48]

The Hohenberg-Kohn total-energy functional for doubly occupied (spin included) electronic states ψ_i can be written

$$E[\{\psi_i\}] = \sum_i \int \psi_i{}^*[-\frac{\hbar^2}{2m}]\nabla^2\psi_i d^3\vec{r} + \int V_{ion}(\vec{r})n(\vec{r})d^3\vec{r} + \frac{e^2}{2}\int\int \frac{n(\vec{r})n(\vec{r'})}{|\vec{r}-\vec{r'}|}d^3\vec{r}d^3\vec{r'} + E_{XC}[n(\vec{r})] + E_{ion}(R_I) \tag{2.11}$$

where E_{ion} is the Coulomb energy associated with interactions among the ions at positions R_I, V_{ion} is the static potential due to ions acting on electrons, $n(\vec{r})$ is the electron density and E_{XC} is the exchange-correlation energy functional, which is also a functional of electron density. Electron density $n(\vec{r})$ is given by,

$$n(\vec{r}) = \sum_i |\psi_i(\vec{r})|^2 \tag{2.12}$$

The Kohn-Sham equations that determine the set of wave functions ψ_i originate from the minimization of the total energy functional and they are written as,

$$\left[-\frac{\hbar^2}{2m}\nabla^2 + V_{ion}(\vec{r}) + V_H(\vec{r}) + V_{XC}(\vec{r})\right]\psi_i(\vec{r}) = \varepsilon_i\psi_i(\vec{r}) \tag{2.13}$$

where ψ_i is the wave function of electronic state i, ε_i is the Kohn-Sham eigenvalue, V_H is the Hartree potential given by

$$V_H(\vec{r}) = e^2\int \frac{n(\vec{r'})}{|\vec{r}-\vec{r'}|}d^3\vec{r'} \tag{2.14}$$

and the exchange-correlation potential V_{XC} is given formally by the functional derivative

$$V_{XC}(\vec{r}) = \frac{\delta E_{XC}[n(\vec{r})]}{\delta n(\vec{r})} \tag{2.15}$$

The Kohn-Sham equations represent a mapping of the interacting many electron system onto a system of noninteracting electrons moving in an effective potential due to all the other electrons.[29] The Kohn-Sham equations are solved self-consistently such that the occupied electronic states generate the charge density which is used to construct the equations. The sum of the Kohn-Sham eigenvalues do not give the total energy, as it was in like the Hartree-Fock method, but the highest occupied eigenvalue in a calculation is nearly the unrelaxed ionization energy for that system.[49]

2.2.3 Pseudopotential Approximation

The third approximation is to be made to the potential of the nuclei. The electrons which lie near the nuclei or in other words, in the lower lying states are strongly bound to the atom and have insignificant effect on the properties of the physical system that elements are involved, except that they shield the potential of the nuclei. These electrons are called core electrons. The pseudopotential theory, developed by Philips and Kleinman 1950; Heine and Cohen 1907[41]; allows one to replace the strong electron ion potential with a much weaker potential- a pseudopotential- that describes all the salient features of a valence electron moving through the solid, including relativistic effects. Thus the original solid system consisting of nuclei, core electrons and valence electrons is now replaced by pseudo valence electrons and pseudo-ion cores. These pseudopotentials are exactly the same outside the core region but are much weaker inside the core region (Fig 2.4). This smoothness of the pseudopotential enormously simplifies the task of solving the Schrödinger equation using a relatively small set of plane waves as basis.

The pseudopotential is constructed, ideally, so that its scattering properties or phase shifts are identical to the all-electron potential but it does not have radial nodes in the core region. Outside the core region the two potentials are identical, and scattering from the two potentials are indistinguishable.

We have used the ultrasoft pseudopotentials generated by the Vanderbilt

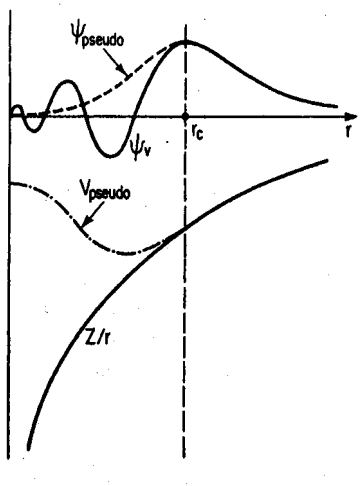

Figure 2.4: Schematic illustration of all-electron (solid lines) and pseudoelectron (dashed lines) potentials and their corresponding wavefunctions. The radius at which all-electron and pseudopotential values match is designated r_c. [Ref 29]

method[42]. These ultrasoft potentials for carbon, aluminum and other metal atoms are usable in every system consisting of these materials but the most accurate results occur whence the system in hand is made of a large number of atoms. The pseudopotentials is only an approximation to the all-electron system, thus extensive analysis and stringent tests are required before using it in predictive studies. We have made some check runs for this purpose and compared our results with experimental or other theoretical results. Among them are comparison of the carbon bulk structure parameters and carbon nanotube lattice constants with experimental findings.

2.2.4 Supercell Method and k-points Sampling

The fourth approximation is the supercell approximation, which allows one to deal with aperiodic configurations of atoms within the frame work of Bloch's theorem. One simply constructs a large unit cell containing the configuration in question and repeats it periodically throughout space. This way, one can use the

plane wave basis and Bloch's wave functions as solutions to the system as if it is periodic.

Bloch's theorem states that in a periodic solid each electronic wave function may be written as;

$$\psi_{\vec{k}} = u_{\vec{k}}(\vec{r}) \ \exp(i\vec{k}.\vec{r}) \tag{2.16}$$

where $u_{\vec{k}}$ is the cell-periodic part, which can be extended using a basis set consisting of discrete set of plane waves whose wave vectors are reciprocal lattice vectors of the crystal,

$$u_{\vec{k}} = \sum_{\vec{G}} c_{\vec{G}} \ \exp(i\vec{G}.\vec{r}) \tag{2.17}$$

where the reciprocal lattice vectors $\vec{G}$ are defined by $\vec{G}.\vec{l} = 2\ \pi$m where $\vec{l}$ is a lattice vector and m is an integer. Therefore the electronic wavefunction can be written as a sum of plane waves,

$$\psi_{\vec{k}} = \sum_{\vec{G}} c_{\vec{k}+\vec{G}} \ \exp[i(\vec{k}+\vec{G}).\vec{r}] \tag{2.18}$$

In our study, we used the supercell method to calculate the electronic structure of non-periodic structure of the nanotube. Nanotubes have periodicity only in the z-direction and along its circumference, but have no periodicity in directions extending outward from the tube axis. In order make the system periodic, we devise a supercell that contains one or two unit cells of nanotube plus the metal atoms around it, depending on the system we intend to investigate. Thus, we have obtained a superstructure formed of these supercells and the basis of this superstructure consists of nanotube plus metal atom. In this superstructure, the distance between adjacent nanotubes is determined such that the interaction between them is negligible. The supercell has a length of $22A^o$ in x- and y-directions, and has the length of one or twice of the lattice vector of the nanotube, that is $4.26A^o$'s. One may check the validity of the size of the supercell by iteratively investigating the interaction between neighboring structure, like forces

or charge distributions. We have conducted a series of calculations for $15A^o$, $20A^o$ and $22A^o$ sizes and the change in the total energy of the system fall below 0.1eV between $20A^o$ and $22A^o$'s, which is a good convergence for such systems.

The vectors $\vec{k}$, which are the wave vectors of the electrons are determined by the boundary conditions that apply to the periodic system, which might also be made periodic using supercell method. For an infinite electron system, the electrons are accounted by an infinite number of $\vec{k}$-points, which correspond to different states in the wave vector representation of the wave functions. The occupied states at each $\vec{k}$-point contribute to the electronic potential in the bulk solid so that, in principle, an infinite number of $\vec{k}$-points are needed to compute this potential. However, the electronic wave functions at $\vec{k}$-points that are very close together will be almost identical. Hence it is possible to represent the wave functions over a region of $\vec{k}$ space by the wave functions at a single $\vec{k}$-point. So, it is possible to calculate electronic potential by only a finite amount of special $\vec{k}$-points, which reside inside the Brillouin zone. We have used the method by Monkhorst and Pack[43] to determine the special $\vec{k}$-points.

The error due to inadequacy of the $\vec{k}$-point sampling can always be reduced by using a higher number of $\vec{k}$-points. The computed total energy using a set of points will converge as the number of $\vec{k}$-points used increases. However, the computational effort required to calculate with high number of $\vec{k}$-points get tremendously high because of the number of plane waves used as basis increases with it. Fortunately, it is possible to iteratively test the dependence of total energy on number of $\vec{k}$-points to determine the minimum number for required accuracy. We have used 6 $\vec{k}$-points in (2x1) supercells, where (2x1) designates two unit cells of nanotube is involved; and 12 $\vec{k}$-points in (1x1) supercells. This number is along the z-direction, where there is real periodicity for the system, but along the x- and y-directions only one $\vec{k}$-point will suffice.

2.2.5 Plane Wave Representation of Kohn-Sham Equations and Energy Cutoff

The Kohn-Sham equations, written in the plane-wave representation can be cast into the following form,

$$\sum_{G'}[\frac{\hbar^2}{2m}|\vec{k}+\vec{G}|^2\delta_{GG'}+V_{ion}(\vec{G}-\vec{G'})+V_H(\vec{G}-\vec{G'}) \\ +V_{XC}(\vec{G}-\vec{G'})]c_{i,\vec{k}+\vec{G'}}=\varepsilon_i c_{i,\vec{k}+\vec{G}} \tag{2.19}$$

In this secular equation, the kinetic energy term is diagonal and the potential are described in their Fourier transforms. The terms in the brackets above is the matrix elements of Hamiltonian, $H_{\vec{k}+\vec{G},\vec{k}+\vec{G'}}$. The size of the Hamiltonian matrix is determined by the choice of the upper limit of $|\vec{k}+\vec{G}|^2$. This limit introduces the term cutoff energy, which is $(\hbar^2/2m)|\vec{k}+\vec{G_c}|^2$, giving maximum kinetic energy of the plane wave to be used. Note that the plane waves with higher energies are required to describe systems with sharp potential peaks. The use of pseudopotentials allows use of smaller cutoff energies thus the size of the Hamiltonian matrix can be controllable. In our studies, a cutoff energy of 300eV sufficed for all the ultrasoft pseudopotentials we used.

2.2.6 Structural Optimization

Most of the time, the stable form of the system we are interested in is not known a-priori. We might want to find the electronic structure, binding energies, phonon modes etc. but they all depend on the geometric structure of the system. The term structural minimization or relaxation refers to minimizing the total energy and the forces acting on ions by moving them around.

The force, in modern physics point of view, is nothing but the gradient of the potential. It is in the direction of the steepest descent of the potential energy at any instant. The first, natural method one must follow when trying to make structural minimization is as follows : Find the forces acting on any ion at an

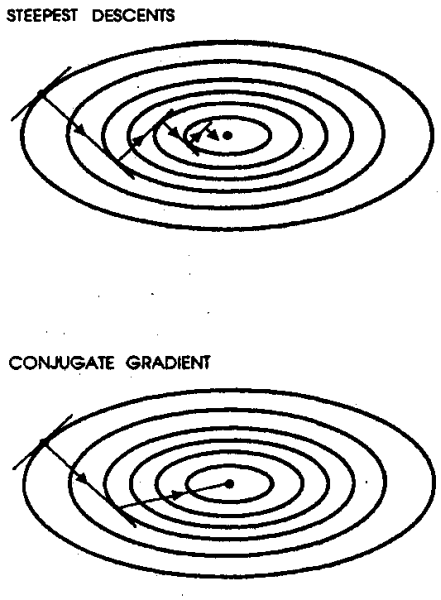

Figure 2.5: The geometrical comparison of the steepest descent method and the conjugate gradient method

instant, and move the atoms in the direction of force with a distance proportional to the magnitude of force. After that, recalculate the energy and forces, and move them again until the forces acting on the ions or the change in energy after each ionic step is negligible.

While it seems acceptable, the steepest descent method described above takes considerably large number of steps to reach the minimum since every direct gradient move contains an error with respect to the ideal final position and the error is carried on to the next step. Another method, named conjugate gradients method, resolves the problem of error transfer between successive steps such that these steps are independent of each other.

2.3 The VASP Program

During our study, we have utilized the VASP (Vienna Ab-Initial Simulation Program) written by G. Kresse and J. Furthmuller[50,51]. This program calculates the total energy of the system and conducts structural minimization. The iterative matrix diagonalization techniques, Broyden broadining, Pulay stress calculations, residual vector minimization method, PAW approximation method and others methods may be followed from the references.[52]

Chapter 3

COVERAGE OF SWNT's BY METAL ATOMS

The problem of interest for this thesis, as already stated in the introduction, is the metal coating and metallization of carbon nanotubes. Metal-nanotube interactions are then naturally at the focus of our interest. These interactions not only cover single atom-tube interactions but also the interactions between metal structures and tubes. Here I shall remark that metal structures might form only around nanotubes or might exist themselves and interact with the tube. The distinction between two statements should be looked over in the light of the importance of metal-metal interactions, when they are collimated around the tube.

The stated importance of metal-metal interactions have in fact crucial role on the possible metal structure formations, for example on uniform coverage of metal atoms around nanotubes.[26,27] At those studies, it was shown that some atoms tended to form clusters or islands of metal atoms while some uniformly distributed themselves over the nanotube. Indeed, we chose to investigate aluminum among the metals which collimated about each other, to analyze whether it would be possible to obtain a stable structure of aluminum around the tube. Our assumption was that the stability of metal structures themselves will effect the metal structure-tube interaction.

In the view of our aim, the important and initial step of analysis began with single atom absorption on carbon nanotubes. We naturally expect, as of in all material interactions, to see differences between the interactions of various metal atoms and the nanotube, depending on their electronic structures. The most basic and fundamental understanding will stem from the analysis of the binding energies for various atoms at various binding sites on the nanotube.

The nanotube is a practically infinite system compared to the size of a single atom. In a (8,0) nanotube of about 1μm length, there are $\sim$30000 carbon atoms, thus calculation of a absolutely single atom on a nanotube is imposible. However, one may consider a periodic system engineered in such way that physically speaking the system is indistinguishable to the system in question up to a vanishing order. It is possible to find details of the method of supercells in Chapter 2. In summary, it is sufficient to take the distance between two atoms in the periodic structure more than 8 A^o. This is not just an assumption though. This choice of interatomic distance is verified by the analysis electronic structure of the periodic system which involves only the (aluminum) atoms placed at the positions they shall reside in the absorption sites. The band structure of this system gives quite flat bands, which are energy states of single non-interacting atoms, not a chain of atoms. On the other hand, a single atom absorption on a nanotube is a barely observable thing, since when nanotube is exposed, many atoms will get absorbed; therefore the supercell method shall yield more realistic results. Considering all those, we chose a two carbon nanotube unitcell (double cell) for our calculations, that is c_{sc}, the length of supercell in z-direction is 2c. c is the lattice parameter of the (8,0) tube along the tube axis. The supercell is a tetragon of sides (x,y,z) of 22 A^o,22 A^o and 8.52 A^o. The number of **k-points** is 6 and the cut-off energy is 300 eV's. The temperature is taken zero during the structure minimizations, thus phonons and ion velocities are kept out of consideration.

As the basis, we chose the (8,0) zigzag nanotube. This nanotube is most suitable for two reasons. First reason is its size. The most common nanotube produced and used in experiments have radii comparable with (8,0) nanotube, of

radius 3.1 A^o. This size is also suitable for computational purposes; the number of atoms inside the supercell containing two primitive cells of bare tube is only 64 and the supercell size is not too big which is that allows use of relatively smaller number of plane waves. The second reason is its semiconducting behavior. The nanotube is not metallic itself, but it can be metallized upon aluminum adsorption.

At first hand, we made a structural minimization for the bare (8,0) CNT and obtained the total energy of this optimized structure. Later, we positioned an aluminum atom at a tentative position over the tube. The exact distance between atom and tube was unknown to us so we also made structural optimization for these systems. Again, please refer to Chapter 2 for details about total energy calculations and structural minimization. Finally, we made single atom and aluminum structure total energy calculations. All the energy calculations are carried out in the same supercell structure.

3.1 Single Atom Adsorption on SWNT

When an atom gets near the carbon nanotube, the electronic structure of both systems are modified and a new structure is formed. From the quantum mechanical point of view, there is a group of possible end states in which the energy of the new structure is lower then the original system where the atom is far from the tube. We might, for the sake of final analysis, omit the intermediate states through which the atom plus nanotube system may pass. The stability of these systems should be understood in terms of minimums on the Born-Oppenheimer surfaces, in which these possible final systems coincide. Thus, an atom might end up in any of stable configurations. The atom might even hop between these states whence it has non-zero thermal excitation energy.

The calculation of the total energy of those end states will give information about the probability of finding the atom at that state. Hereafter, we shall refer to those states as adsorption sites which are possible positions of aluminum atom with respect to a hexagon of carbon atoms on the nanotube. We have considered

four different adsorption sites; the **H-site** which is above the center of hexagon, the **Z-** and **B-sites** which are above the zigzag and axial C-C bonds, and finally the **T-sites** which are on top of the carbon atoms. (Fig 3.1)

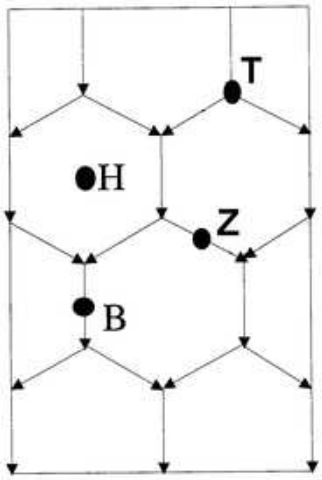

Figure 3.1: Various binding sites over the carbon nanotube. The carbon atoms placed at the edges of the hexagons are not shown.

The reader may verify, upon carefully investigating the figure, that these sites cover all the possible absorption sites except those that lie geometrically between themselves. However, those sites are not stable and eventually end up in any of the four sites.

The binding energy for the adsorbed atom is obtained from the expression,

$$E_b = E_T[SWNT] + E_T[At] - E_T[At + SWNT] \tag{3.1}$$

in terms of the total energies of the fully optimized bare nanotube (E_T[SWNT]), the single atom (E_T[At]), and the atom adsorbed on nanotube system (E_T[At+SWNT]). The binding energies for various stable adsorption sites are then positive.

The binding energies of various atoms on the nanotube is given in Table 3.1, with respect to different adsorption sites. The difference between binding energies of atoms is significant, more over the difference between binding energies of the same atom may differ very much depending on the adsorption site.

Atoms	Binding Energies (eV)			
	H-site	**B-site**	**Z-site**	**T-site**
Al	1.740	1.608	1.542	N/A
Ti	3.804	3.160	2.932	2.859
Ni	2.266	2.416	2.419	2.285
Fe	2.798	2.366	2.834	1.789
Cu	0.575	0.881	0.711	N/A
Au	neg.	<0.1	<0.1	neg.

Table 3.1: The binding energies of atoms at various adsorption sites. N/A corresponds to unstable binding, that is atom initially at that site moved to other sites. neg. is negligible amount of binding energy.

We have found that the binding of Al and Cu at the **T-sites** are unstable; the adatoms move to other sites upon relaxation. The step-by-step analysis (snap shot investigation for each ionic step) showed that once the symmetry is broken, the atom moved towards the **B-site** in case of aluminum and eventually ended in **H-site**, or towards **Z-site** in case of copper.

The most stable binding occurs at the highest binding energy site. The high binding energy makes us think that the interaction is chemical in nature. Therefore a large amount of charge rearrangements and transfers might have occurred between the adatom and tube. In order to verify this, we made extensive analysis of electronic structure. The Mulliken analysis for aluminum, which is calculation of total charge around ions inside a definite radius, has yielded a charge transfer of about $0.7e^-$ from aluminum atom to the nanotube. The interaction between gold (Au) and nanotube is then presumably of physisorbtion, that is no charge transfer occurs but instead Coulombic interaction lowers the energies of the individual systems.

The band structures for Ti and Au [see Fig 3.2], at the opposite site of binding energy profile, yield that Ti has charge transfer or sharing with nanotube where Au only introduces a state in the bandgap. The state of titanium mixes with the nanotube energy states and the electronic structure of the nanotube is

also modified. One may see this in the hybridization of the conduction band of the tube, compared to the virtually unaffected band structure of Au adsorbed nanotube band structure.

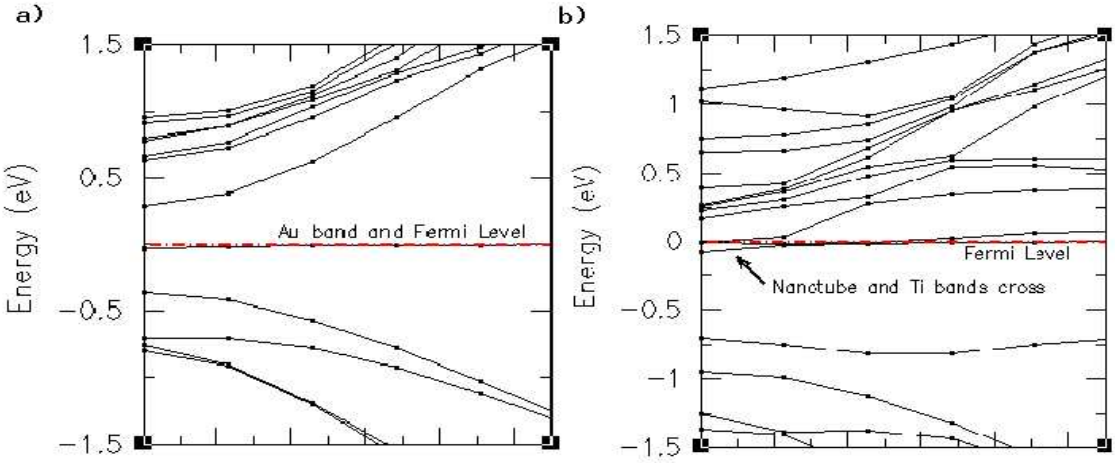

Figure 3.2: (a) The band structure of Au at **B-site** (b) The band structure of Ti at **H-site**. Zero of the energy is taken at the Fermi level shown by dash-dotted lines.

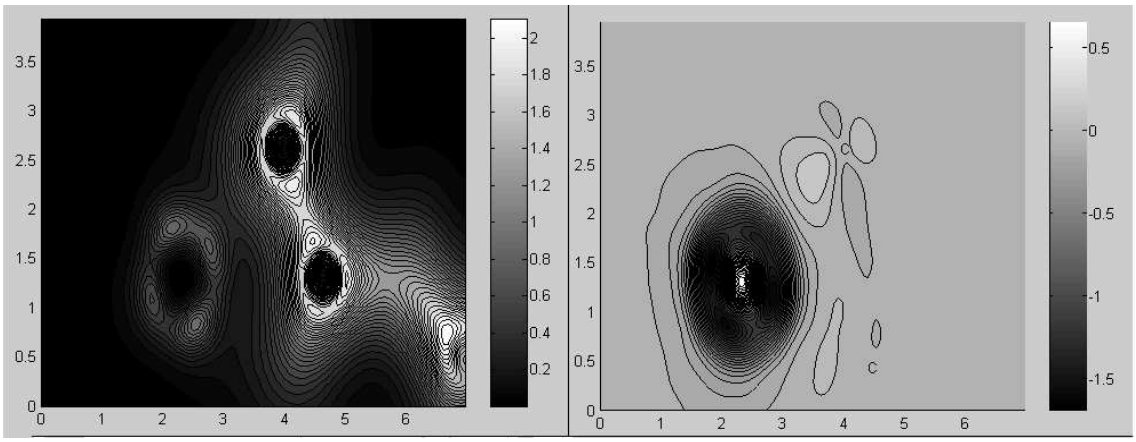

Figure 3.3: The charge density contour plots for Ti atom adsorbed on **H-site**. (Left) The total charge density plot. The lighter regions indicate higher electron density. The carbon-carbon bound is clearly visible. (Right) Difference charge density plot. The darker regions indicate loss of electron, light regions indicate gain of electron.

The strength of the titanium-nanotube interaction is an interesting issue. More interesting maybe, is the difference between the binding energies for various sites. The difference suggests that the interaction strength depends on the orbitals mainly involved.

We have made charge density analysis for the titanium bound to the **H-site** [see Fig 3.3]. Calculation of the difference charge density requires various steps. First of all, we have calculated the charge densities of the titanium only atom, the nanotube only structure and the titanium adsorbed nanotube system all in the same supercell. In that calculations, we kept the positions of the atoms precisely the same with the adsorbed complex system. After we have obtained the real space charge density distribution of these three systems, we have extrapolated the charge density into a reciprocal space, or momentum space using fast Fourier transform algorithms. It is possible to obtain very smooth charge density over any region in space once you obtain the projection to the reciprocal space by applying back Fourier transform.

We have chosen a plane that passes through the centers of the titanium atom and two carbon atoms and calculated the charge density of three systems over that plane. The charge transfer $\triangle\rho$ is calculated as,

$$\Delta\rho = \rho_{Ti+SWNT}(\vec{r}) - \rho_{Ti}(\vec{r}) - \rho_{SWNT}(\vec{r}) \tag{3.2}$$

The electron density in the d orbital of titanium is lowered, as one may understand from the spherical distribution of the lost charge and that charge is transferred to nearby carbon atoms. The interaction is somewhat localized but the charge in the carbon-carbon bound is also increased so it effects the electronic structure of the whole nanotube system. Indeed, the system becomes metallic upon adsorption.

The interaction is not as strong for other binding sites of titanium. The reason we suggest for that is the importance of the d orbital interaction, which geometrically occurs the most in **H-site**. This idea may be generalized in the way that atoms with large amount of d orbital valence electrons shall show strong interaction with nanotube, which is in fact the case for transition metal elements.

At this point, it is also important to remark the high binding energies of the iron and nickel atoms, which are both transition metals.

The binding energy of aluminum is negligible (<0.1 eV, even negative) on the graphite surface. Remember that nanotube is generated by rolling a sheet of graphite into a cylinder. The reason of a significant binding to the nanotube may be explained as that the orbitals are rearranged due to the curvature to contribute to the binding interaction[16,34,40]. The π-bonds extending both inwards and outwards in the graphite surface are disturbed when the system is curved due to interaction (repulsion) between electrons in π-bonds standing inside the tube, thus the chemical activity of the outward extensions increase with $\pi^* - \sigma^*$ hybridization.

3.2 Aluminum Structures on SWNT

After having discussed the adsorption of a single Al atom, we moved to the adsorption of several Al atoms, where the Al-Al interactions play an important role. This is the step where we consider the interaction between tube and aluminum structures. Eventually, we expected to observe that single atom-tube interaction to be drastically different from aluminum structure-tube interaction, in view of the stability problems for the structure.

Besides, we aimed to observe a full metal coverage of nanotube, at the end paving the way to the formation of a nanowire with significant metallic behavior. This would not only be interesting by its physical nature and probable technological innovations, but also the presence of a stable uniform coverage while experiments observed non-uniform coverage[25,26] for aluminum would be interesting itself.

Since the binding energy at the **H-site** is the largest, we first considered a coverage where all Al atoms are placed at the **H-sites**. We started with a quarter coverage case (i.e. Θ=0.25) by placing eight Al atoms at the hollow sites around the circumference forming a ring in the double cell of the (8,0) nanotube. (Fig 3.4) In this initial structure, the C-Al and Al-Al distances are 3.7 A^o and 2.4 A^o

respectively. In the supercell method, the distance between two successive rings in each supercell is about 8.52 A^o, so the rings may be considered as indepentdent from each other.

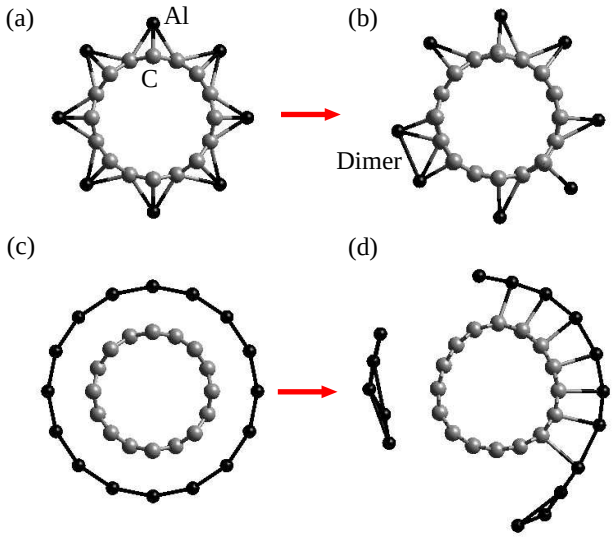

Figure 3.4: (a) Initial structure of the Al ring where the adatoms were placed at **H-sites** on the circumference of the tube (b) Dimerization upon relaxation of Al atoms starting from structure shown in (a). (c) The initial structure of the uniform coverage of a nanotube where all **H-sites** are occupied by Al atoms (d) The nucleation of isolated Al clusters from the initial structure shown in (c) Both relaxed structures shown in (b) and (d) are not final structures, but they are intermediate configurations toward a 3D cluster formation.

The initial configuration is then relaxed. The relaxation process, as described in Chapter 2, finally brings the system into a stable configuration, that is the forces acting on all individual atoms are below a certain value. We tracked the path of atoms during their relaxation, taking snapshots at about every ten steps and observed that the atoms moved in a sort of hysteresis in the initial phase of motion. The reason is that the system possessed a good symmetry in the initial configuration thus forces acting on atoms were in equilibrium. However, slightest deviations from symmetry resulted in forces that disturb the system.

After the relaxation, we found that some of the Al atoms moved away from the nanotube surface, towards their neighboring Al atoms. These atoms eventually

form a dimer, as observed in Fig 3.4(a)→Fig 3.4(b). The distance between the Al atoms that form the dimer is 2.1 A^o. The carbon atoms remained very close to their initial positions because while nanotube is easy to deform, it is also elastic and preserves its shape and geometry in order to lower its energy. The aluminum atoms are more free to move, since the energy landscape through which they travel is not steep, which might be understood from small differences between binding energies of various adsorption sites. The discussion of this dimerization process is left to Chapter 4, however briefly stating, we attribute this to the strength of Al-Al interaction compared to Al-nanotube interactions.

The instability of the **H-site** ring structure was an initial test to cover nanotube with aluminum atoms. The next logical step was to apply uniform coverage. The uniform half-coverage (i.e., Θ=0.5), where initially all **H-sites** are occupied by Al atoms (i.e. , 32 C and 16 Al atoms) also exhibits instability. We have again taken snapshots of the system at various instances during the relaxation. The Al atoms again exhibited hysteresis upon initial relaxation. Once the symmetry is broken, the atoms began moving towards each other. The Al atoms tend to decrease the Al-Al distance from 3.0 A^o to 2.5-2.8 A^o, and at the same time they rise above the surface of the nanotube, that is, move radially outward from the center of hexagon. At the end, small and isolated clusters form on the nanotube. Some of the adatoms become completely disconnected from the surface to initiate a 3D island growth. In other words, the aluminum atoms prefer to form 3D aluminum structure instead of staying adsorbed to the nanotube. This situation is illustrated in Fig 3.4(c)→3.4(d).

In accordance to our aim, investigation of metal-nanotube interaction and metal coverage of nanotube, we decided to continue our investigation with other structures. The similarity between the investigated and newly proposed structures was inevitable since the stability condition imposes a certain symmetry on the aluminum structure. For that reason, we made crucial changes in our hypothetical configurations keeping in mind that the strength of metal-metal interaction plays a very important role in the final stability of the system. Our point was based on two facts : First, the Al-Al and Al-nanotube interactions

should be optimized simultaneously. This way those interactions will not work against each other. Second, which is strongly related to first one, that the aluminum structure around the tube should have a more or less stable structure itself. In fact, the configurations we generated in the light of those assumptions led to stable systems, each important and crucial in themselves.

3.3 Stable Aluminum Structures around Nanotube

3.3.1 Metal Nanoring around SWNT

Here I first discuss the zigzag Al nanoring coverage, which is obtained by placing Al atoms on top of carbon atoms (**T-sites**), forming a zigzag ring [see Fig 3.5]. This structure includes 64 C and 16 Al atoms in the double unit cell. In this initial configuration the Al-Al distance is $2.33\,A^o$, and the angle of Al-Al-Al bond is 137^o. After structure optimization, the ring shape preserved itself and the structure was stable, that is all the forces on the system and the total energy converged within $< 0.1\,eV/A^o$ and $1 \times 10^{-4} eV$, respectively. After the structure optimization is completed, the Al-Al bond length is increased to $2.56\,A^o$, Al-Al-Al bond length is decreased to 124^o, yielding the radius of the nanoring to be $5.9\,A^o$. A side view of the optimized structure of Al nanoring wrapping the (8,0) SWNT is illustrated in Fig 3.5.

The interaction between nanotube and zigzag ring of Al atoms also moved the Al atoms from their **T-sites** positions to nearly **B-sites** positions. Remember that as we earlier stated, the bindings of Al atoms at **T-sites** are not stable but atoms moved to **H-sites** upon relaxation. Here however, atoms tended to move toward the **B-sites**.

We have further analyzed the SWNT-Al nanoring interaction by studying the effect of rigid displacement (u) and rotation (ϕ) of the nanoring around the tube axis. The variation of the energy as a function of energy was calculated for various steps of displacement and rotation. The energy variation with respect to

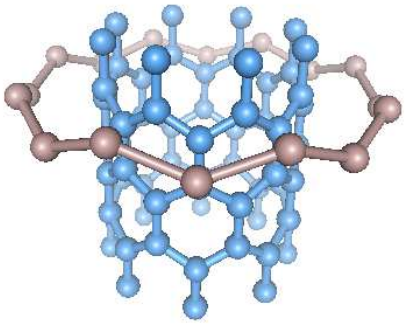

Figure 3.5: Zigzag ring of Al atoms, formed by placing Al atoms at the **T-sites**, over the carbon atoms. There are 16 Al atoms for 64 C atoms in this configuration, forming a ring, which led to stable structure after relaxation. Observe that the Al-Al distance is nearly halved compared to the unstable ring structure that led to dimerization.

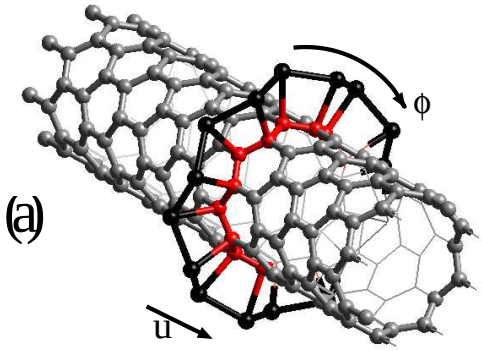

Figure 3.6: A view of the optimized structure of Al zigzag nanoring formed on a (8,0) SWNT.

rigid displacement is calculated as,

$$E(u) = E_T^u[Al + SWNT] - E_T[Al + SWNT] \tag{3.3}$$

where $E_T^u[Al + SWNT]$ is the total energy of the unrelaxed tube-ring system with the ring displaced by u. The highest energy configuration (energetically least favourable) corresponds to the situation where Al atoms are close to the **H-sites**. For u=c, that is the ring is displaced by the unit cell distance along the tube axis [see Fig 3.7], the energy is $0.7\,eV$ higher then the optimized structure, $E(u = 0)$. This is strange at first sight because what this translation

is nothing but moving all atoms to the same positions on the next nanotube cell. However, the positions of the carbon atoms there are different because no structural relaxation was carried at that site. This is another strong indication of the interaction between nanotube and ring because the geometric modification of nanotube atom configuration occured and it plays important role in lowering energy.

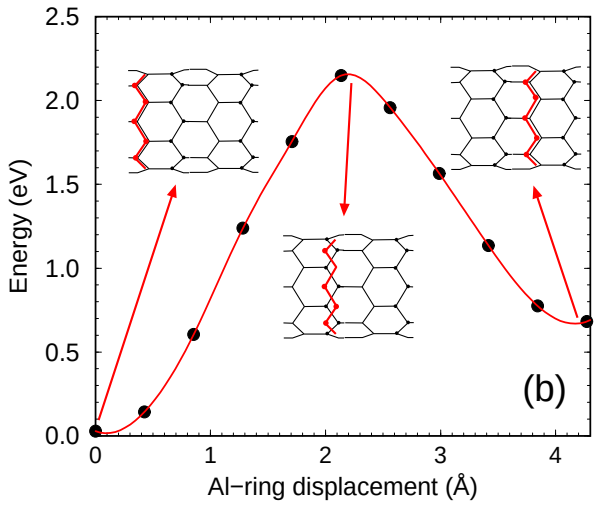

Figure 3.7: Variation of the (relative) energy with the rigid displacement u of the Al ring along the tube axis. The starting point is the optimized structure. The insets show schematic views of the nanoring (thick gray lines) and a carbon nanotube for three particular configurations.

The energy dependence of the system with respect to a rigid rotation about the tube axis is shown in Fig 3.8. The rotation angle ϕ was changed in the interval $-22.5^o<\phi<22.5^o$. The highest energy configuration again corresponds to the case where Al atoms are closest to **H-sites**. The rotation dependence has a double-minimum potential separated by a barrier of $0.2eV$.

The two tests we have conducted has proved that the system of zigzag nanoring around the tube is a low energy configuration with respect to motion of ring about the nanotube. Indeed, the binding energy of nanoring to nanotube is $0.85\,eV$. All those tests signify that once the ring is formed around the tube, it possesses stability.

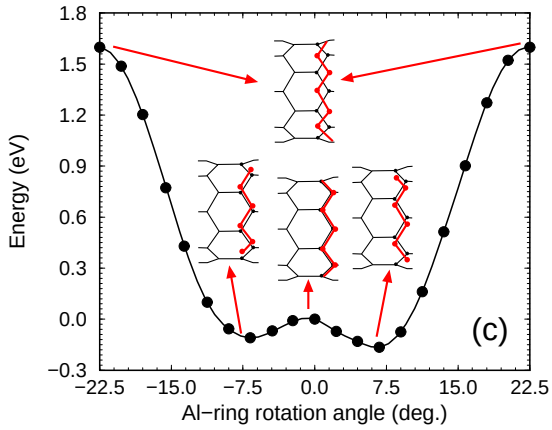

Figure 3.8: Variation of the energy with rigid rotation ϕ of the Al ring around the nanotube. The right minimum at ϕ=7^o corresponds to the optimized structure; ϕ=0^o is the ideal configuration, with atoms aligned perfectly on top of carbon atoms.

What about the stability of the ring itself? Was the aluminum ring stable itself apart from the nanotube? Our calculations showed that the ring structure was also stable!

We took the ring of aluminum atom in the same supercell, this time removing the carbon atoms from the system but keeping the Al atoms at the same positions. Before relaxation, we carried out force analysis on the atoms and it showed that the forces were already small. The relaxation preserved the zigzag shape of the ring and increased the radius of the system from 5.9 A^o to 6.0 A^o. The Al-Al-Al angle increased to 131^o but Al-Al distance was kept nearly the same, 2.57 A^o on the average. Thus, apart from some minor geometric modifications, the zigzag ring structure was stable alone. The binding energy per atom in that ring was about 1.9 eV.

The electronic properties of the zigzag Al nanoring around nanotube system is quite interesting and it may lead to important applications. We have made band structure and density of states analysis for the nanotube, nanoring around nanotube and bare nanoring. We aimed to compare and investigate these results and understand the result of interaction on these systems. The band structures for all three systems is shown in Fig 3.9.

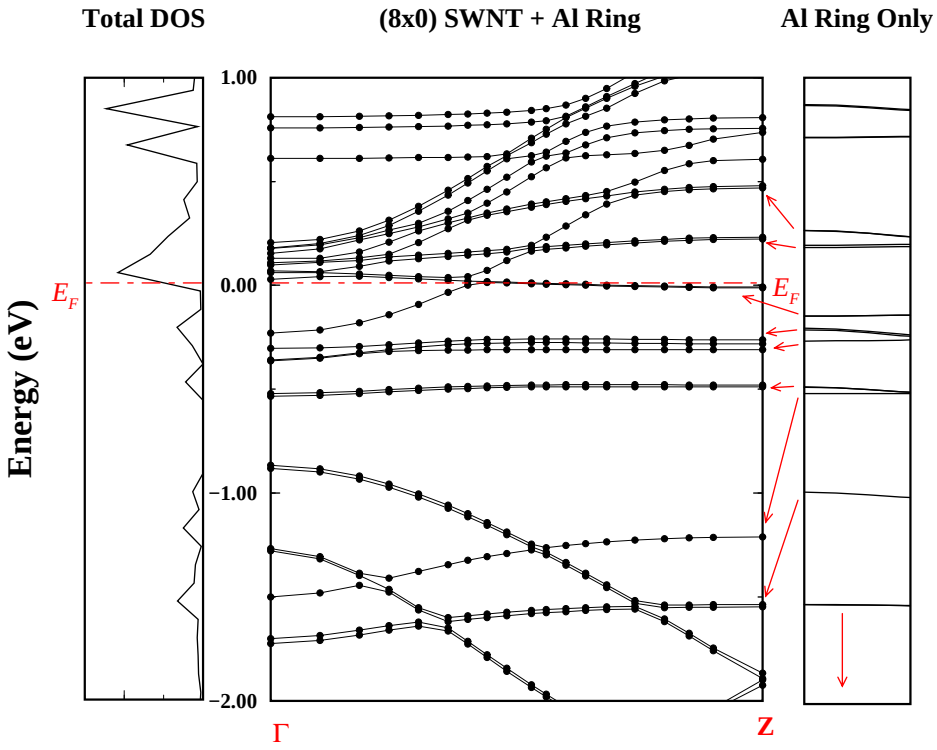

Figure 3.9: The energy bands along the nanotube axis of the Al nanoring formed on (8,0) SWNT (middle panel). The total density of states is shown in the left panel. The right panel shows the energy levels of the bare Al nanoring. The zero energy is taken at the Fermi level.

The (8,0) SWNT is a semiconducting nanotube, with a band gap of about $0.59\,eV$. The band structure yields that the nanotube plus metal nanoring system is metallic. The metallicity of the system occurs since the Fermi level crosses more then one bands and those bands are half-filled. Thus, there is an empty state which it can occupy, so conductance is possible.

The band structure of the bare nanoring is made of discrete energy levels. This is what we expect, because the ring system, although it has periodicity on the circumference, has no periodicity in the z-direction and it is like a molecular system instead of a crystal. Thus, the electrons occupy molecular orbital like states with discrete energies. However, there is very slight dispersion among these bands due to otherwise negligible interaction between rings in neighboring

supercells. The important point though, is not this. The metallicity of the new complex system stems from the mixing of the bare aluminum ring and bare nanotube states. The lowest energy band in the conduction region which is empty in bare nanotube is half-filled by electrons taken from the ring. Observe Fig 3.8 to see the mixing of bands. The arrows originating from bare nanoring bands show where these bands ended up in the complex system. The crossing of aluminum and nanotube bands at the Fermi level show that there is a charge transfer from the ring to the nanotube. Mulliken analysis indicates that 0.15 electrons are transferred from each Al to the nanotube system.

The resulting metallicity due to band mixing brings out an important application because we now have a metallic ring of nanometer radius around a robust template, the SWNT. The electronic wave function forms a circular shape passing over the ring plane, which indicates conductance along the circumference.

3.3.2 Metal Nanotube

Finally, I shall present another stable uniform coverage, which is obtained from 16 Al atoms placed at alternating **T-sites** in one unit cell. This corresponds to half coverage (i.e., θ=0.5). It is also valid to name the configuration as an aluminum nanotube around carbon nanotube [see Fig 3.10]. The radius of this tube is 5.6 A^o. This tube is like a wrapping of aluminum two dimensional sheet into a cylinder.

Upon relaxation of the system, Al atoms moved toward the **B-sites**, while they preserved the tubular structure. The Al-Al nearest neighbor distance is 2.7 A^o (which is close to that of the bulk Al nearest neighbor distance, d_o=2.8 A^o) and the Al-tube distance is 2.4 A^o. View this relaxation as a sliding of tubes in reverse directions. This structure is a metal with a finite density of states at the Fermi level (Fig 3.10(b)).

The aluminum nanotube alone was relaxed under the same conditions, with the same unit cell, after removing the carbon nanotube. The relaxed metal nanotube has kept its geometry, with just a small radius change to 5.4 A^o. This

stable aluminum nanotube is the first nanotube that was ever found in the literature. The aluminum nanotube demonstrates metallicity as expected.

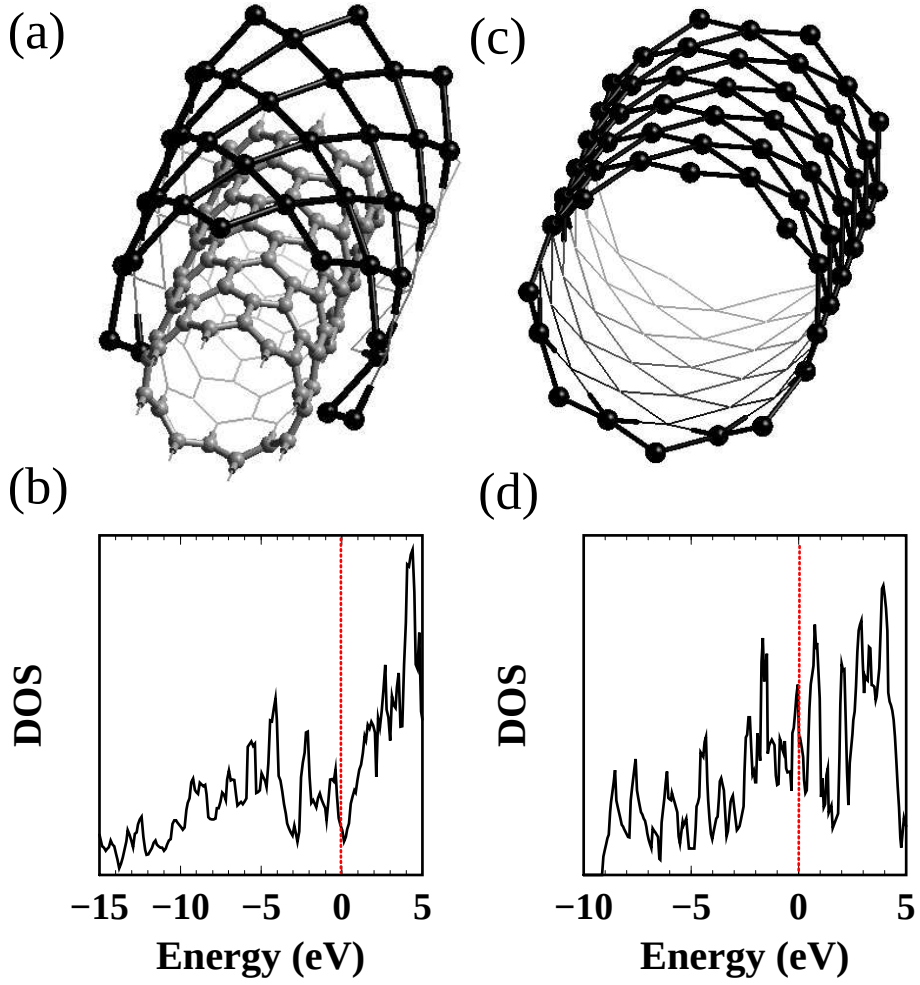

Figure 3.10: (a) Aluminum nanotube (dark) around a SWNT (grey). (b) Total density of states for an Al nanotube + SWNT structure. (c) Structure of an Al nanotube alone, which is also stable with a smaller radius (d) Total density of states for the Al nanotube shown in (c). The zero energy is taken at E_F.

Chapter 4

DISCUSSION AND CONCLUSION

In this thesis, we presented our study about the metal-nanotube interaction. I have deliberately chosen to put the discussions on the results to a separate section because they are all interdependent. The main objective of the thesis study was to understand the aspects of metal structure formation around the nanotube and/or the coverage of nanotube by metals. The program of the study was as follows : We started single atom Al and Ti calculations, meanwhile we planned for various structures and coverage types on nanotubes. Single atom runs showed that Ti had a higher binding energy compared to Al. This information was in accordance with the experimental findings by Zhang *et al.*[26,27], which reported that Ti coated nanotubes uniformly while Al formed bead like structures and clusteres. After a short time, the series of long calculations started earlier showed that the aluminum atoms put in a ring at **H-sites**, where they bound the strongest, formed dimers and eventually the ring structure was broken. The uniform half-coverage study yielded a similar result; the symmetry of the system was broken, the aluminum atoms moved away from the surface and clustered to form disconnected islands. These results were no surprise, since as a widely accepted idea, the uniformity of coverage of any surface by a material depends on the strength of interactions between the surface and material and between the elements forming the material itself.

At this point, it is best to present the details of the results we obtained that

verifies the assumption : The stability of coverage of nanotube by aluminum was not possible because the aluminum-aluminum interactions disturbed the system. In the **H-site** aluminum ring, as referred before, the forces between the two neighboring Al atoms were higher then the forces that kept them at the original sites. The system could not maintain its geometry while it balanced the forces at the same time. Due to this, the aluminum atoms moved away from the well that they resided, which also disturbed the nanotube. And once the aluminum atoms got closer, they formed dimers and the nanotube relaxed itself back, eventually further weakening the tube-atom interaction.

The same thing happened in the uniform half-coverage trial. Aluminum atoms moved away from the **H-sites** and nucleated to form islands. The tendency to get apart from the surface is a result of nothing but the forces on atoms from other Al atoms. The 3D structure that eventually formed is a low energy structure for these atoms.

While it seems that the stability or uniformity is not possible because sooner or later the aluminum-aluminum interaction will overcome the nanotube-aluminum interaction, the picture is not yet complete. What structure does the aluminum atoms really tend to? The answer is as follows : They are trying to form structures that are themselves similar to aluminum only structures, that is their form in the absence of nanotube resembles the aluminum structure in one, two or three dimensions.

The first-principles calculations predicted linear chain, planar zigzag and various other structures for stable Al wires[53,54]. The Al-Al distance for the linear chain in those studies is $2.2\,A^o$, which is closer to the length of the dimer bond. Hence, the Al-Al distance in the **H-site** ring was large for stable configuration. In order to visualize the picture, one may consider the ring shape as the planar zigzag chain wrapped around to form the ring. In the bulk aluminum, the Al-Al distance is $2.5\,A^o$. Remember that the Al distance changed from $3.0\,A^o$ to 2.4-$2.5\,A^o$ upon relaxation of the uniform half-coverage structure, or in other words, got closer to bulk structure parameters.

This discussion led us to consider a new aspect in our structure trials. If we

can not get over the force of aluminum-aluminum interaction, then it was best to use it for our sake. The idea in a few items is that, if

- the aluminum structure around the tube would be stable itself
- the nanotube-aluminum interactions would not be against the aluminum-aluminum interactions

then it might be possible to obtain stable metal structures around the nanotube.

It was not so difficult to satisfy the first condition. We had tried a zigzag ring of Al made of 16 atoms as the initial structure. It was shown that Al has a zigzag linear chain structure, and the Al-Al distance is $2.53\,A^o$. Indeed, the resultant zigzag ring is very similar to the predicted structure. The second condition was also satisfied by putting the aluminum atoms at the **T-sites**. At these sites, the atoms are nearly free to move so aluminum-aluminum interaction would not be against the tube-aluminum interaction. Moreover, the bare aluminum was stable.

The metal nanotube configuration we finally tried was also satisfying the two conditions for stability. The observation of the stability of metal tube was a very interesting finding because it is the first time ever reporting of a solely metal nanotube. The metal tube was stable and had a radius smaller than the radius it had around the nanotube. Thus, the metal tube alone might prefer to shrink but the forces that would lead to shrinking is not against the tube interaction and preserves symmetry. Besides, the atoms also had mobility over the surface so they did not have to give up their interactions with the tube, as they had to do in the case for **H-site** trial. The fact that all atoms move towards the **B-sites** indicate that these aluminum structures interact with the nanotube. In fact, the rotation and displacement tests for the zigzag ring demonstrate this interaction.

There is still one more important point to deliberate, which will extend our criteria on uniform coverage and stability of metals to other atoms other then aluminum. The titanium atoms definitely have strong binding to the nanotube, shown in single atom calculations. And it has a good uniform coverage around the nanotube. But what about iron? Fe atoms also bind to the nanotube very strongly, but iron does not exhibit uniform coverage around the tube [again refer

to Refs. 25,26]. This fact has an important thing to say : The covering atoms may interact strongly with the tube, but the interaction between each other and the stability of the final metallic structure is the crucial aspect for uniform coverage.

The metal nanoring and metal nanotube structures we demonstrated deserve a few more words on them. The nanoring is a conducting ring and it might carry ballistic current. This might give rise to persistent currents over it, which can be used to detect or create magnetic fields. Clearly, this is a very promising effect for many nanodevice applications, and provides tools for experiments on fundamental aspects of quantum mechanics. The metal nanotube on the other hand, can do more like carrying large currents along the axis of tube, and it might be considered as a perfect molecular wire (or nanowire). The current carrying capacity of the wire united with interesting physical properties of the nanotube bring out a very capable candidate for molecular electronics.

The experimental evidence for the nanoring and metal nanotube is not yet shown, and will most probably be a challenge for a long time. We do not claim that these structures occur spontaneously. As stated many times, the initial configurations are deliberately chosen. However, the nanotube may serve as a template for these structures. Moreover, aluminum is not the best choice for such devices, titanium for example has better coverage. Our study on the other hand had demonstrated the possibility of these structures and we try to explain the criteria for metal coverage and stability of structures. We assume that the advances in the technology will allow fabrication of such novel structures.

Finally, I would like to discuss the single-atom results. The binding energies of the transition metal elements are quite high. We attribute this to the role played by the localized, symmetric d orbital electrons. The strong dependence of the binding energy to the adsorption sites also support the idea that binding strength is related to the orbitals involved in interactions.

In conclusion, we can itemize what we have contributed in this thesis as follows :

- We have calculated the binding energies over nanotube of single atoms of Ti, Fe, Ni, Al, Cu and Au, in the order of decreasing binding energies.

We have shown that transition metal elements have strong binding to the nanotubes and the binding strength is related to the adsorption sites or in other words, to the orbitals involved in reactions.

- We have observed that the uniform coverage of nanotubes by aluminum may not be possible due to the strong metal-metal interactions, which is stronger then metal-tube interactions. But we also found that the metal-metal interaction may lead to stable structures forming around the tube.

- For the first time ever, we have observed formation of stable metal nanoring and metal nanotube around carbon nanotubes. We have seen that these structures are stable themselves, without the presence of carbon nanotube. We also showed that the metal nanoring interacts strongly with the nanotube. Both metal ring and tube plus nanotube structures are metallic.

- Finally, we have proposed a criteria for uniform metal coverage of the nanotube. We state that it might be possible whence the metal structure formed around tube is stable itself and the metal-metal interactions are not against the metal-tube interactions.

In last words, we investigated the metal-tube interaction. This field is very open to new researches. We would be just too pleased to see our results used as a basis for further discussions.

Bibliography

[1] R. Kubo, 1977. (private communication to M.Endo)

[2] M. S. Dresselhaus, G. Dresselhaus, and P. C. Eklund, University of Pennsylvania Workshop (August 1991)

[3] J. W. Mintmire, B. I. Dunlap, C. T. White, Phys. Rev. Lett. **68**, 631 (1992)

[4] S. Iijima, Nature (London) **354**, 56 (1991)

[5] Treacy *et al.*, Nature **381**, 678 (1996)

[6] S. A. Chesnokov, V. A. Nalimova, A. G. Rinzler and R. E. Smalley, Phys. Rev. Lett. **82**, 343 (1999)

[7] W. G. Wildöer *et al.*, Nature (London) **391**, 59 (1998); T. W. Odom *et al.*, *ibid.* **391**, 62 (1998)

[8] R. Saito *et al.*, Phys. Rev. B **53**, 2044 (1996); J. C. Charlier *et al.*, *ibid.* **53**, 11 108 (1996).

[9] L. Chico *et al.*, Phys. Rev. Lett. **76**, 971 (1996); **81**, 1287 (1998)

[10] C. Park, Y. H. Kim and K. J. Chang, Phys. Rev. B **60**, 10656 (1999)

[11] C. Kilic, S. Ciraci, O. Gülseren and T. Yildirim, Phys. Rev. B **62**, 346 (2000)

[12] O. Gulseren, T. Yildirim, S. Ciraci and C. Kilic (to be published)

[13] C. Dekker, Physics Today **52**, 22 (1999)

[14] H. Dai *et al.* Nature **384**, 147 (1996)

[15] S. B. Aranson *et al.*, Appl. Phys. Lett. **75**, 2842 (1999)

[16] O. Gulseren, T. Yildirim and S. Ciraci, Phys. Rev. Lett. **87**, 116802 (2001)

[17] S. J. Tans, A. R. M. Verschueren and C. Dekker, Nature **393**, 49 (1998)

[18] Martel *et al.*, Appl. Phys. Lett. **73**, 2447 (1998)

[19] Ebbesen *et al.*, Nature **382**,54 (1996)

[20] H. Dai, E. W. Wong, C. M. Lieber, Science **272**, 523 (1996)

[21] Tombler *et al.*, Nature **405**, 769 (2000)

[22] Kane *et al.*, Europhys. Lett. **41**, 683 (1998)

[23] A. Bezryadin, A. R. M. Verschueren, S. J. Tans and C. Dekker, Phys. Rev. Lett. **80**, 4036 (1998)

[24] J. Tersoff, Appl. Phys. Lett. **74**, 2122 (1999)

[25] C. Zhou, J, Kong, H. Dai, Phys. Rev. Lett. **84**, 5604 (2000)

[26] Y. Zhang, N. W. Franklin, R. J. Chen, H. Dai, Chem. Phys. Lett. **331**, 35 (2000)

[27] Y. Zhang, H. Dai, Appl. Phys. Lett. **77**, 3015 (2000)

[28] K. L. Chopra, *Thin Film Phenomena*, McGraw-Hill, Newyork (1969)

[29] M. C. Payne, M. P. Teter, D. C. Allen, T. A. Arias, and J. D. Joannopoulos, Rev. Mod. Phys. **64**, 1045 (1992)

[30] P. Hohenberg, W. Kohn, Phys. Rev. B **136**, 864 (1964)

[31] W. Kohn, L. J. Sham, Phys. Rev. A **140**, 1133 (1965)

[32] J. P. Perdew and Y. Wang, Phys. Rev. B **46**, 6671 (1992)

[33] R. Saito, G. Dresselhaus, M. S. Dresselhaus, *Physical Properties of Carbon Nanotubes* (London : Imperial College Press, 1998)

[34] O. Gulseren, T. Yildirim, and S. Ciraci, Phys. Rev. B **65**,155410 (2002); **65**,153405 (2002)

[35] S. Iijima and T. iclihashi, Nature **363**, 603 (1993)

[36] Bethune *et al.*, Nature **363**, 605 (1993)

[37] Thess *et al.*, Science **273**, 483 (1996)

[38] Falvo *et al.*, Nature **385** (1997)

[39] Soh *et al.*, Appl. Phys. Lett. **75**, 627 (1999)

[40] T. Yildirim, O. Gulseren, and S. Ciraci, Phys. Rev. B **64**, 075404 (2001)

[41] J. C. Philips, Phys. Rev. **112**, 685 (1958); M. L. Cohen, V. Heine, Solid State Physics **24**, 37 (1970)

[42] D. Vanderbilt, Phys. Rev. B **41**, 7892 (1990)

[43] H. J. Monkhorst, and J. D. Pack, Phys. Rev. B **13**, 5188 (1976)

[44] P. Hohenberg, and W. Kohn, Phys. Rev. **136**, 864B (1964)

[45] W. Kohn, and L. J. Sham, Phys. Rev. **140**, 1133A (1965)

[46] W. A. Harrison, *Solid State Theory* (Tokyo : McGraw-Hill Company, 1970)

[47] E. P. Wigner, Trans Faraday Soc. **34**, 678 (1938); L. Hedin, and B. Lundqvist, J. Phys. C **4**, 2064 (1971); S. Vosko *et al.*, Canadian J. Phys. **58**, 1200 (1980); J. P. Perdew, and A. Zunger, Phys. Rev. B **23**, 5048 (1981)

[48] J. P. Perdew, and Y. Wang, Phys. Rev. B **46**, 6671 (1992)

[49] Perdew *et al.*, Phys. Rev. Lett. **49**, 1691 (1982)

[50] G. Kresse, and J. Furthmuller, Comput. Mat. Sci. **6**, 15 (1996)

[51] G. Kresse, and J. Furthmuller, Phys. Rev. B **54**,11169 (1996)

[52] Bylander *et al.*, Phys. Rev. B **42**,1394 (1990); Teter *et al.*, Phys. Rev. B **40**, 12255 (1989); Arias *et al.*, Phys. Rev. B **45**,1538 (1992); P. Pulay, Chem. Phys. Lett. **73**,393 (1980); P. E. Bloechl, Phys. Rev. B **50**, 17953 (1994)

[53] D. S. Portal *et al.*, Phys. Rev. Lett. **83**, 3884 (1999)

[54] P. Sen, S. Ciraci, A. Buldum and I. Batra, Phys. Rev. B **64**, 195420 (2001)